# Kinetic and thermodynamic studies for the sorptive removal of crude oil spills using a low-cost chitosan-poly (butyl acrylate) grafted copolymer

Ahmed M. Omer[a,*], Randa E. Khalifa[a,*], Tamer M. Tamer[a], Ahmed A. Ali[b], Yossry A. Ammar[c], Mohamed S. Mohy Eldin[a]

[a]_Polymer Materials Research Department, Advanced Technologies and New Materials Research Institute (ATNMRI), City of Scientific Research and Technological Applications (SRTA-City), New Borg El-Arab City, P.O. Box: 21934 Alexandria, Egypt, Tel./Fax: +2034593414; emails: Randaghonim@gmail.com (R.E. Khalifa), Ahmedabwahed@yahoo.com/Ahmedomer_81@yahoo.com (A.M. Omer), ttamer85@yahoo.com (T.M. Tamer), mohyeldinmohamed@gmail.com (M.S.M. Eldin)_
[b]_Egyptian General Petroleum Corporation (EGPC), Egypt_
[c]_Chemistry Department, Faculty of Science, Al-Azhar University, Egypt, email: yossry@yahoo.com (Y.A. Ammar)_

**ABSTRACT**

In this study, a low-cost chitosan (CS) marine biopolymer was grafted with oleophilic butyl acrylate (ButA) monomer for the sorptive removal of crude oil spills from the water surface. Fourier-transform infrared spectroscopy and scanning electron microscope analysis were used for investigating the chemical structure as well as the surface morphology of CS-g-poly (ButA) copolymer. The dependency of oil-sorption capacity on parameters such as sorption time, crude oil concentration, sorbent dosage, agitation rate, and sorption temperature was considered. The empirical equilibrium data were verified using different isotherm models. The results clarified that both Langmuir and Freundlich isotherm had an exceptional agreement with the laboratory data. The maximum monolayer adsorption capacity was 27.7 g/g for native CS, while it reached a maximum value 83.3 g/g for the grafted copolymer. The kinetic characteristics of the adsorptive performance were undertaken by practising several models. The results validated that the sorption regarded the pseudo-second-order model and film-diffusion-controlled mechanism. Besides, the thermodynamic parameters endorsed the process to be endothermic, favorable and spontaneous. The gained results advocate the excellent potential of the developed chitosan grafted copolymer as oil-sorbent materials for oil spill clean-up applications.

_Keywords;_ Chitosan; Butyl Acrylate; Oil spill removal; Kinetics; Isotherm; Thermodynamics

## 1. Introduction

Recently, cleaning water resources contaminated by oil from routine shipping, dumping, industry or oil spillage is a great challenge to the environmental scientists. Spilt oil may evaporate, disperses or form a slick layer in water or accumulates and submerges [1,2]. The presence of carcinogens polycyclic aromatic compounds and dissolved crude oil components in water possess severe environmental threats to the aquatic system. It may also affect human life through skin, inhalation and eye irritation; besides it devastates the economy [3,4]. The adverse influences of oil spills worldwide calls for a crucial need to develop an extensive range of materials for the treatment of contaminated areas effectively and generate an increasing interest about the new cleaning up routines [5,6]. The essential representative methods used for combating spilt oil was classified as

* Corresponding author.

biological and chemical, physical and mechanical methods [7,8]. Adsorbent materials have been considered the most traditional solution is owing to their proficiency to collect, remove and recover the whole oil spills via the adsorption, or the absorption mechanism, or both (sorption) [9,10]. Natural sorbents are reliable, rapid, available, biodegradable, and renewable [3]. However, the hydrophilic character and the little oil absorbency are the main drawbacks with these natural sorbents [11]. For decades many researchers are focused on the development of natural materials for the potential use as sorbents for the significant oil spill removal [4,12]. For instance, Sidik et al. [13] have been used lauric acid to enhance the hydrophobicity of oil palm leaves]. Hydroxypropyl cellulose acrylate has also been synthesized by Keshawy et al. [11] as oil sorbent.

Additionally, Sokker et al. [14] have been illustrating the affinity of the synthesized chitosan-based polyacrylamide by radiation induced-graft polymerization toward oil adsorption. Developing the cellulosic structures as composites [15], fibrils [16,17], and graft copolymers [18] have been also investigated. Latterly, Mohy Eldin et al. [19,20] reported significant hot issues to concern the improvement of chitosan and its modified forms either Schiff base and grafted copolymer as superior sorbents for the removal of oil spills from the water surface.

Chitosan (CS) is a naturally cationic polysaccharide provided by the incomplete deacetylation of chitin elicited from the Crustacean's shells chemically. It is consists of regurgitated built-in units of ß-(1→4)-2-acetamido-2-deoxy-d-glucopyranose and Regular-(1→4)-2-amino-2-deoxy-d-glucopyranose [21,22]. Owing to its prominent unique features [23] such as a high concentration of hydroxyl and amino groups, non-toxicity, biocompatibility, bio-degradability, easily shaped into different forms and lower cost, it has a significant potential to treat water from numerous pollutants [24,25]. Nonetheless, CS has a lower interior surface area and can agglomerate in its natural form as a gels. Also, the recycling complexity during the sorption process due to their solubility in the acidic medium is a significant disadvantage [19]. These obstacles lessen the rate of sorption and the supreme sorption capacity. However, it can be minimized by the chemical and physical modification via the creation of new derivatives having outstanding hydrophilic and hydrophobic characters. Grafting of vinyl monomers such as methyl methacrylate, acrylamide, acrylic acid, and N-isopropyl-acrylamide onto the abounding hydroxyl and amine groups on the CS backbone through grafting copolymerization is a promising and effective modification method [26]. The resultant covalently bonded grafted functional CS derivatives have high chelating and improving sorption properties [27]. Grafting polymer chains on CS can be attained by many techniques [28] as γ-radiation, ring-opening, free-radical and cationic polymerization (grafting to and grafting from). The objective of this research is to fabricate low-cost commercial CS grafted with ButA monomers via a free-radical polymerization process. Accomplished CS-g-poly (ButA) copolymers were characterized by Fourier-transform infrared spectroscopy (FTIR) and scanning electron microscope (SEM) analysis. Factors influencing the sorption process such as the time intervals, initial crude oil concentration, sorbent dose, agitation rate and temperature were investigated. Furthermore, sorption kinetics, isotherms and thermodynamics of heavy crude oil on CS and its grafted copolymers were also interpreted.

## 2. Experimental section

### 2.1. Materials

Shrimp shells were accumulated from marine restaurants in Alexandria (Egypt). N-butyl acrylate (ButA; 98%) and potassium persulfate (KPS; 99%) were provided by Sigma-Aldrich (Germany). Hydrochloric acid (HCl; 37%), sodium hydroxide (NaOH; 99%), acetic acid (CH$_3$COOH; 98%), and ethanol (C$_2$H$_5$OH; 99%) were obtained from El-Nasr Company (Egypt). Heavy Land Egyptian crude oil delivered from Belayem Petroleum Company (Egypt).

### 2.2. Methods

#### 2.2.1. Preparation of chitosan

In brief, chitin was firstly extracted from the shrimp shells by scattering in 5% HCl in ratio 1:14 (w/v) at 25°C and left overnight, following by rinsing in distilled water to get free of acid and calcium chloride. The resulted in de-mineralized shells were then treated with 5% NaOH in ratio 12:1 (v/w) for 24 h at 25°C, collected and washed several times till neutrality. The final product was recognized as pure chitin. Thereafter, CS was obtained via deacetylation of chitin using 50% (w/v) NaOH in ratio 1:50 (w/w) for 12 h, at 100°C–120°C. The provided CS was washed and dried at 40°C, and eventually, refined by dissolving in 2% (w/v) acetic acid overnight then filtered and precipitated in 5% (w/v) NaOH. The concluding product was gathered and washed to exclude the extra NaOH [19,20].

#### 2.2.2. Preparation of chitosan-poly (butyl acrylate) grafted copolymer

CS-g–poly (ButA) copolymer was fabricated regarded to the author's previous work [20] by dissolving CS (0.2 g) in 2% acetic acid (20 mL) at 25°C followed by dropwise addition of ethanol (10 mL) under vigorous stirring. To the CS solution 0.1 g, KPS dissolved in 50 mL distilled water was added with raising the temperature to 60°C. Accurately, was 10 and 20 mL of ButA (78 and 156 mM) was simultaneously injected slowly after 20 min with a supplementary portion of 0.05 g KPS dissolved in 5 mL distilled water. The produced precipitate acquired from the grafting reaction after 3 h was recovered upon centrifugation. The grafted copolymer was then washed repetitively for 2 h with acetone and methanol using soxhlet. Then dried at 50°C to exclude the ButA homopolymer. The grafting percentage (GP %) was calculated according to the following equations [29]:

$$GP(\%) = \left[ \frac{(W_1 - W_0)}{W_0} \right] \times 100 \tag{1}$$

where $W_0$ and $W_1$ represent weights of CS and the resultant grafted copolymer.

*2.3. Characterization*

The chemical characteristics of the synthesised CS and CS-g-poly (ButA) copolymers were investigated by Fourier-transform infrared (FTIR) spectroscopy (Shimadzu FTIR - 8400 S, Japan). Moreover, the degree of deacetylation (DD) of CS was estimated from IR spectrum via the peak area (A) measurement [30]. Also, the surface morphologies of the prepared samples were observed with a scanning electron microscope (SEM, Joel Jsm 6360LA, Japan).

*2.4. Batch oil sorption experiments*

All the sorption experiments of heavy crude oil from the oil/water system was conducted using 0.1 g adsorbent per 300 mL of artificial seawater (distilled water contains 3.5% NaCl). The prepared solution was agitated in a shaker incubator at a speed of 100 ppm for an anticipated period at room temperature. Factors affecting the sorption kinetics and equilibrium behaviours, such as the effect of the initial oil concentration (8.33–50) g/L and the mentioned contact time (10–240) min, were examined. Further, the variety of additional affecting parameters on the batch sorption process such as sorbent dose (0.1–1) g, agitation rate (50–200) rpm, and the temperature 25°C–40°C were also studied. The sorption capacity was calculated according to the standard method (ASTM F726-99) [31] as follows:

$$\text{Oil sorption capacity}\,(\text{g/g}) = \frac{\left(W_s - W_w - W_0\right)}{W_0} \qquad (2)$$

where $W_s$, $W_w$, and $W_0$ are the weight of the saturated sorbent (water + oil + sorbent), the weight of the absorbed water, and the initial dry weight of the sorbent in-unit g, respectively. The quantity of absorbed water was determined through the extraction separation using *n*-hexane as the solvent.

# 3. Results and discussion

As presented in Table 1 the deacetylation degree (DD %) of chitosan was 91%, while the grafting percentage (GP %) of the grafted copolymers was 68% and 88% for CS-g-poly (ButA10) and CS-g-poly(ButA20). Increasing GP % value with increasing ButA content in the feed mixture could be ascribed to the high availability of ButA at the initiated active sides on CS backbone. This action results in enhancing the grafted amount of poly (ButA) and thus, the grafting percentage value increases accordingly [20,32]. However, a variation of the grafting percentage referred to the different affinity of the CS matrices

Table 1
Values of DD and GP (%) for native CS and its grafted copolymers

| Sample | DD (%) | GP (%) |
|---|---|---|
| CS | 91 | 0.0 |
| CS-g-poly (ButA10) | 91 | 68.0 |
| CS-g-poly (ButA20) | 91 | 88.5 |

towards the polymerization solution components; water and ethanol. It also has impacts on the homogeneity of the monomer and the polymer phase.

*3.1. FTIR spectra*

Fig. 1a represents the FTIR chart of CS and CS-g-poly (ButA) copolymers. The FTIR spectrum explains the systematic bands of CS, that is, the stretching vibration of OH and NH$_2$ groups illustrated by broadband within 3,200–3,600 cm$^{-1}$. Also, the bending O–H at 1,394 cm$^{-1}$ specifies the presence of OH groups. The weak absorption peak between 2,835–2,950 cm$^{-1}$ (C–H stretch) distinguishes the methyl and methylene groups. The typical peak at 1,620 cm$^{-1}$ refers to the NH–C=O and C=O stretching vibration, and the peaks at 1,066–1,059 cm$^{-1}$ assigned to the C–O–H. On the other hand, FTIR spectra of the CS-g-poly (ButA) copolymers, clarified a significant change confirming grafting [33], that is, the appearance of sharp absorption bands at 1,729 cm$^{-1}$ which ascribed to the C=O group stretching vibration. Also, the absorption bands located at 2,876; 2,930; 1,380; and 1,470 cm$^{-1}$ refers to the C–H stretching vibration and in-plane bending vibration, respectively.

*3.2. SEM analysis*

SEM images of the developed sorbents were shown in Fig. 1b. It was recognized that CS exhibited a rough surface. A significant change in the surface morphology of CS was noticed after the grafting process. Where, a heterogeneous and muddy-like surface with two phases was observed, and this might be attributed to the generated hydrophobic/oleophilic poly butyl-acrylate on the surface of CS [32]. Moreover, the muddy surface of CS-g-poly (ButA20) sample was denser than that of CS-g-poly (ButA10) sample as a result of increasing the grafted amount of poly (ButA) on the surface of CS with increasing ButA monomers content in the feed mixture.

*3.3. Factors affecting sorption equilibrium*

*3.3.1. Effect of sorbent dosage*

Indeed, the impact of the sorbent mass is an essential feature in a broad-scale application in the oil spills clean-up. The outcome of the sorbent dose (0.1–1) g on the sorption capacity was studied with an initial oil concentration of 16.67 g/L at 25°C (Fig. 2a). The figure revealed that a sharp decrease in the sorption capacity befalls with the increase in the sorbent amount. This decline in the sorption capacity is fundamentally attributable to the residual unsaturated active sites during the process. In other words, increasing the sorbent dose at the same crude oil concentration leads to a decrease in the adsorbed amount per unit mass of CS sorbents due to the residence of a limited amount of oil per unit weight of the sorbents. This observation agreed with other relative publications [34,35].

*3.3.2. Effect of the agitation rate*

Considering the influence of shaking speed on the oil adsorption affinity is very essential to reflect weather and

(A)



(B)
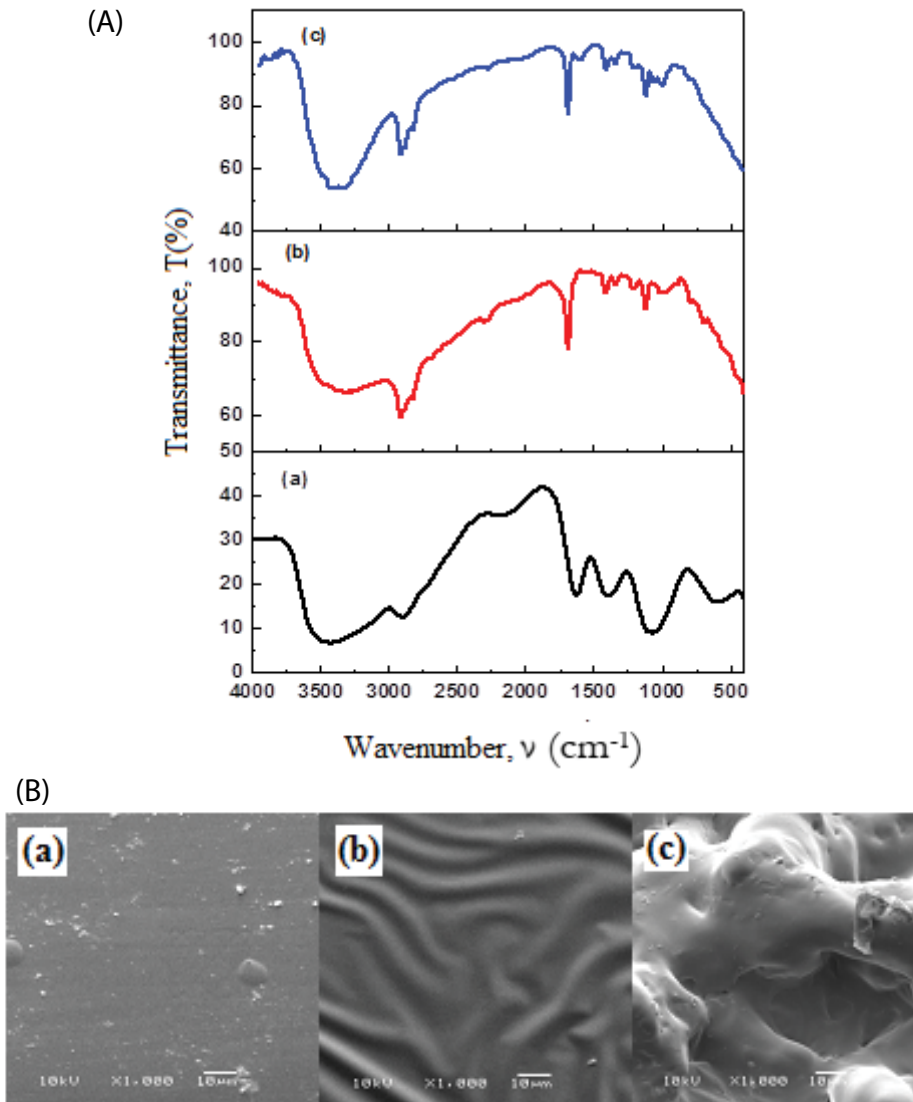


Fig. 1A. FTIR spectra of (a) CS, (b) CS-g-poly (ButA10), and (c) CS-g-poly (ButA20) and 1B. SEM images of (a) CS, (b) CS-g-poly (ButA10), and (c) CS-g-poly (ButA20).

wave conditions in the seawater. Fig. 2b reviews the influence of altering the shaking velocity (50–200) rpm on the sorption capacity. The obtained results reported that improving the shaking speed from 50 to 150 rpm has a positive impact on the sorption capacity for all CS adsorbents. Where, the sorption capacity enhanced from 11 to 18.5, from 28.4 to 41, and from 34 to 44 g/g in case of CS, CS-g-poly (ButA10), and CS-g-poly (ButA20), respectively. These results could be attributed to the enhancement in the oil dispersal and increase the exposed adsorbent surface area to the spilt oil. Besides, rising the agitation speed promotes the dissipation of oil spillage towards the sorbent surface [36]. Oppositely, a further rise in the agitation speed up to 200 rpm creates a reduction in the values of oil sorption capacity. This declining in the oil sorption capacity could be due to a further increase in the agitation velocity exceeding 150 rpm could improve the process of the oil-water emulsion, and as a

consequence, diminish the attraction capabilities between the sorbent and oil molecules and promote the occasion of oil desorption process [37].

### 3.3.3. Effect of contact time and sorption kinetics

The oil sorption rate is an essential key feature for the choice of oil adsorbents. The correlation between the sorption time and crude oil sorption capacity is represented in Fig. 3a. As inferred from the results, the oil sorption capacities of CS and the advanced hydrophobic-oleophilic grafted copolymers rose exponentially with rising the time up to 180 min; next, it begins to decline with a further increase up to 300 min. It was clarified that the beginning oil sorption rates are quite fast; thus, the light oil spills will be absorbed quickly by the prepared sorbents in several minutes upon the adjunct to the artificial seawater. This behavior is owing
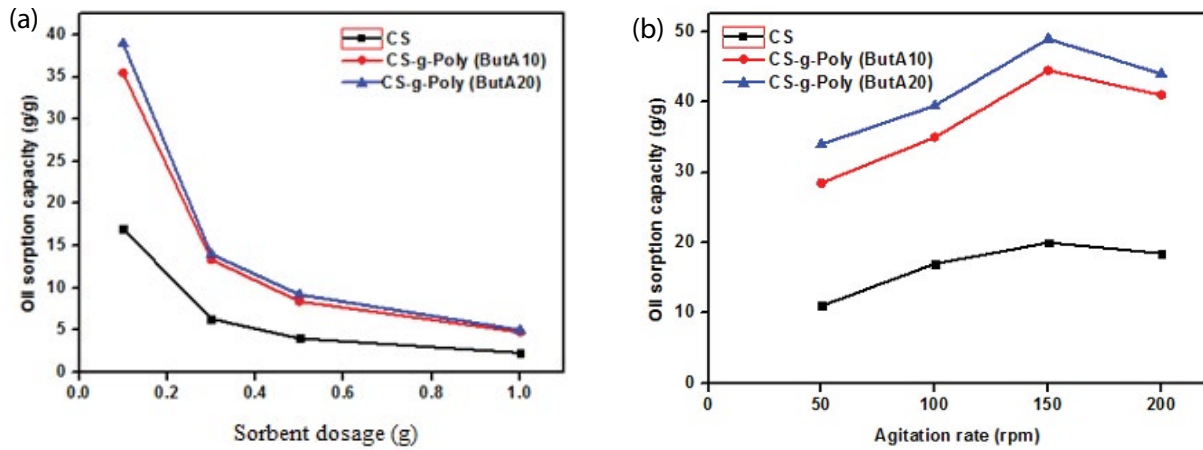
Fig. 2. (a) Effect of the sorbent amount on the crude oil sorption capacity and (b) effect of the agitation rate on the crude oil sorption capacity.

to the interactions of Van der Waals forces and the hydrophobic interaction, which enables the diffusion of extra oil to the interior free sites [38].

Moreover, a considerable number of abandoned surface localities were ready for sorption throughout the initial step, later; the remaining vacant sites were difficulty packed after a lapse of time due to the repellence forces amongst the oil molecules on the solid and bulk phases. Alternatively, with increasing contact time up to 180 min, the diffusion becomes more difficult as the vacant volume within the sorbent decreases. Thus, the attraction between the sorbent and oil molecules decreased. Furthermore, the desorption could occur which; induce a drop in the sorption capability. So, the amount of adsorbed tends to increase somewhat slowly and subsequently reaches a steady state. Further, this sorption rate of CS and its modified grafted copolymers can satisfy the terms of governing the diffusion of leaked oil on the water surface. This investigation is consistent with the findings of other authors [39,40].

To illustrate the reaction pathways of the sorption of CS and its grafted copolymers for crude oil spills, the experimental data were further fitted using the pseudo-first-order (Eq. (3)), the pseudo-second-order (Eqs. (4) and (5)), and the Elovich (Eq. (6)) kinetics models, as symbolized in the following linear forms, respectively [13,39,41]:

$$\ln\left(q_e - q_t\right) = \ln q_e - k_1 t \tag{3}$$

$$\frac{t}{q_t} = \frac{1}{k_2 q_e^2} + \frac{t}{q_e} \tag{4}$$

$$h = k_2 q_e^2 \tag{5}$$

$$q_t = \beta \ln\left(\alpha\beta\right) + \beta \ln t \tag{6}$$

where $q_e$ and $q_t$ (g/g) are the heavy crude oil sorption capacity at equilibrium and time $t$ (min), $k_1$ (min$^{-1}$) and $k_2$ (g/g min) are the constant rate parameters of the pseudo-first-order and the pseudo-second-order sorption. $h$ (mol/g min) is the

initial sorption rate. $\beta$ (g/g) and $\alpha$ (g/g min) are reporting the number of possible adsorptive sites and the sorption extent.

The values of $k_1$ and $k_2$, as well as the equilibrium oil sorption capacity ($q_e$), were determined from the slope and intercept of these plotted curves (Figs. 3b and c). A correlation of the theoretical ($q_{exp}$) and the figured ($q_{cal}$) values of the oil sorption capacity are presented in Table 2. It was deduced that the $q_{cal}$ values of the pseudo-second-order kinetic model are very close to the $q_{exp}$ values while the pseudo-first-order exhibited a prominent difference. Although, the pseudo-first-order and pseudo-second-order models provided fit values of the correlation coefficient (all values of $R^2$ are close to 1). However, the results above manifested that the pseudo-second-order model is more proper for depicting the kinetic sorption model. This observation is consistent with other publications [37,42]. These results imply that the chemisorption mechanism plays a vital role in the sorption process [43]. The adsorbed oil droplets are attached to the sorbent surface by covalent forces as those occurring between the bound atoms in the oil molecules. Further, for the same oil sorption by CS grafted copolymers, the $k_2$ values are also altered. However, the slight difference of the $k_2$ values cannot confirm the increase or decrease of the oil sorption time owing to the actuality of error from high crude oil viscosity [44]. In general, the modification of native CS results in a noteworthy enhancement of the oil sorption rate as it increased from 0.5 to 1.4 mol/g min for CS and CS grafted copolymers beyond the grafting experiment.

The probability that the oil sorption was taking place in the water/oil/CS sorbents system, and comprising the contribution of other forces, besides the regular Vander Waals forces, has been assessed by concerning the Elovich model. It assumes that the actual sorbent surfaces are energetically-heterogeneous [45]. The Elovich equalization does not submit any particular mechanism for the adsorbate–adsorbent reactions. It has comprehensively been established that the chemisorption can be described by this model [42]. The kinetic data plotted in Fig. 3d and the parameters scheduled in Table 2 indicate a good correlation among theoretical lines and the experimental points. In addition, the correlation coefficient, $R^2$ values for CS and its grafted forms
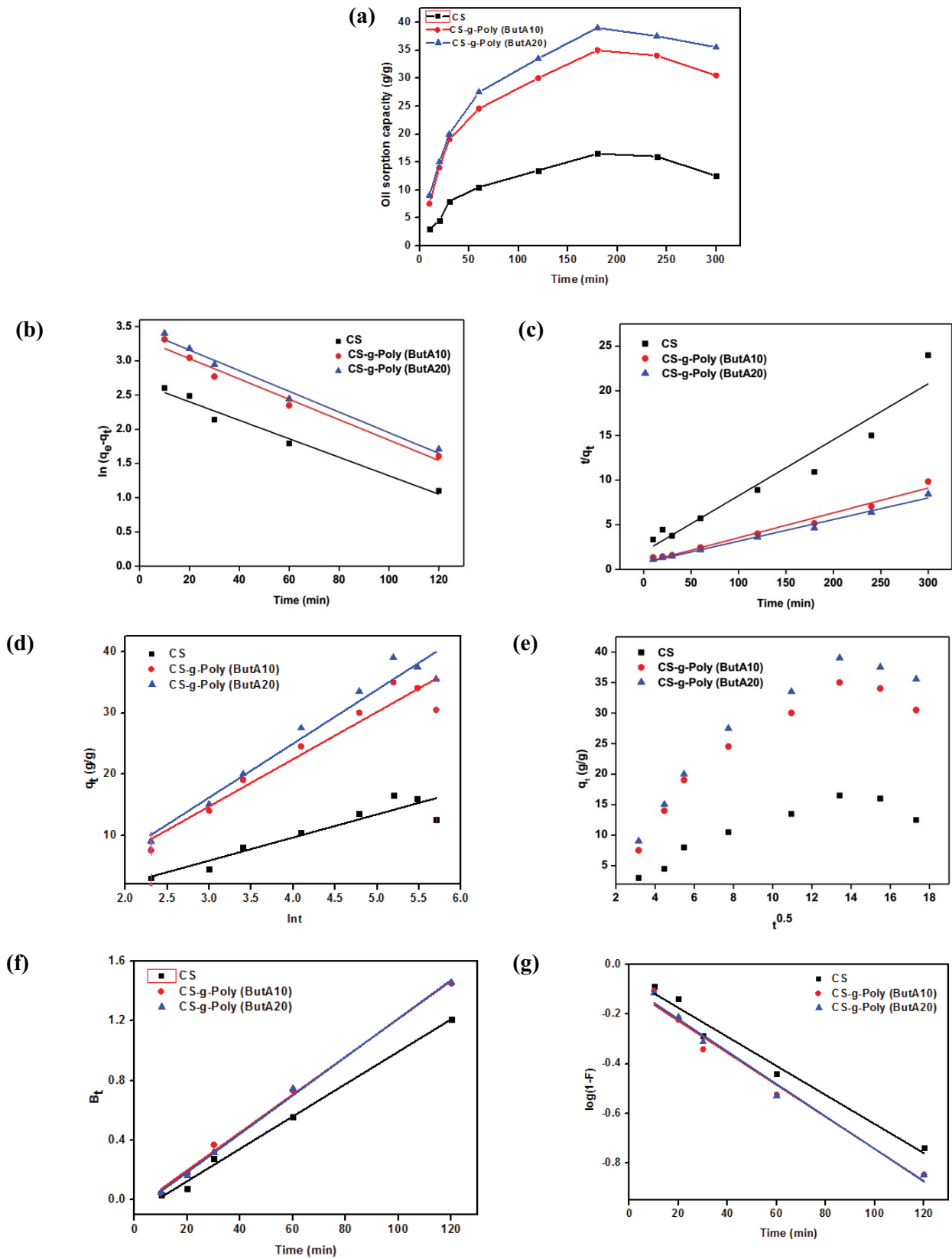
Fig. 3. (a) Effect of the sorption time on the crude oil sorption capacity, (b–g) kinetics models for the sorption of the crude oil onto the prepared chitosan derivatives, (b) pseudo-first-order, (c) pseudo-second-order, (d) simple Elovich, (e) intra-particle diffusion, (f) Boyd, and (g) reconfirmation Boyd model.

were agreed with the $R^2$ values obtained from the pseudo-second-order model. It supposes that the Elovich model well describes the kinetics of the crude oil sorption onto the surface of the CS adsorbents.

The kinetic data were estimated using the intraparticle diffusion (Eq. (7)) and the Boyd model (Eqs. (8)–(10)) describing below to study the diffusion mechanism of crude oil sorption, [13,46]:

$$q_t = K_p t^{0.5} + C \tag{7}$$

$$F = 1 - \frac{6}{\pi^2} \sum_{n=1}^{\infty} \frac{1}{n^2} \exp\left(-n^2 B_t\right) \tag{8}$$

$$B_t = \left( \sqrt{\pi} - \sqrt{\pi - \left(\frac{\pi^2 F}{3}\right)} \right)^2 \quad \text{For } F < 0.85 \tag{9}$$

$$B_t = -0.498 - \ln\left(1 - F\right) \quad \text{For } F > 0.85 \tag{10}$$

where $K_p$ (g/g min) is the intra-particle diffusion rate constant and $C$ is the intercept. $F$ is the fraction of solute adsorbed at any time ($F = q_t/q_e$).

As shown in Fig. 3e, the first, sharper portion is the immediate sorption or exterior surface sorption. The second part is the gradual sorption stage wherever the intraparticle-diffusion is the rate-controlling. Besides, the third portion exists in certain cases; it is the equilibrium stage where the intraparticle diffusion started to slow down as a result of the deficient crude oil concentrations retained in the bulk solutions. The $K_p$ values (Table 2) are 1.14, 2.37, and 2.39 g/g min for CS, CS-g-poly (ButA10), and CS-g-poly (ButA20), successively. This investigation implies that CS grafted copolymers supports improved rate of

crude oil sorption more than native CS and is sequentially interrelated to enhanced bonding as designated by Itodo et al. [47]. Moreover, as can be comprehended from Fig. 3e, none of the linear relationships passed through the origin, that is, ($C > 0$); this deviation might be attributable to the difference in the mass transfer rate from the initial to the final sorption stages. Further, the boundary layer depth is established by the values of the intercept; the larger the intercept, the greater is the boundary layer consequence as represented in Table 2. Itodo et al. [47] reported that the sorption mechanism assumes intraparticle diffusion if the following circumstances are met: (i) High $R^2$ values, (ii) Straight line passing into the origin, and (iii) $C < 0$. A validity investigation which deviates from (ii) and (iii) aforementioned demonstrated that the transport mode is governed with more than one process, which means that two or more steps transpire. Besides, it indicates that the intraparticle-diffusion is not the only rate defining step. This observation is in agreement with other authors [47,48].

On the other hand, the linearizer plot of Boyd equation (Fig. 3f) and its reconfirmation plot (Fig. 3g) were used to distinguish between the film and particle-diffusion controlled sorption [46]. If the plot is a straight line passing through the origin, the sorption rate was governed by particle diffusion; otherwise, it was administrated by the film diffusion. In addition, the slow diffusion of oil molecules leads to slow solvation, indicating that the equilibrium would take a long time. It was observed from the plots that the film-diffusion is the rate-controlling mechanism. Other authors also reviewed related investigations [49,50].

### 3.3.4. Effect of initial oil concentration and sorption isotherms

For the isotherm considerations, the impact of the initial crude oil concentration is examined because the initial

Table 2
Sorption parameters of kinetic models

| Sorbent type | CS | CS-g-poly (ButA10) | CS-g-poly (ButA20) |
|---|---|---|---|
| Kinetic model | Parameter | Values | |
| Pseudo-first-order | $q_{e,cal}$ (g/g) | 7.260 | 9 | 9.400 |
| | $q_{e,exp}$ (g/g) | 16.500 | 35 | 39 |
| | $K_1$ (min$^{-1}$) | 0.013 | 0.015 | 0.015 |
| | $R^2$ | 0.977 | 0.976 | 0.984 |
| Pseudo-second-order | $q_{e,cal}$ (g/g) | 15.900 | 35.800 | 41 |
| | $q_{e,exp}$ (g/g) | 16.500 | 35 | 39 |
| | $K_2$ (g/g min) | 0.002 | 0.001 | 0.001 |
| | $h$ (mol/g min) | 0.500 | 1.320 | 1.390 |
| | $R^2$ | 0.930 | 0.980 | 0.990 |
| Elovich model | $\alpha$ (g/g min) | 1.047 | 0.420 | 0.380 |
| | $\beta$ (g/g) | 4.700 | 3.650 | 3.680 |
| | $R^2$ | 0.980 | 0.990 | 0.990 |
| Intraparticle diffusion | $C$ | 0.618 | 3.530 | 3.250 |
| | $K_p$ | 1.140 | 2.370 | 2.390 |
| | $R^2$ | 1.000 | 0.990 | 0.990 |
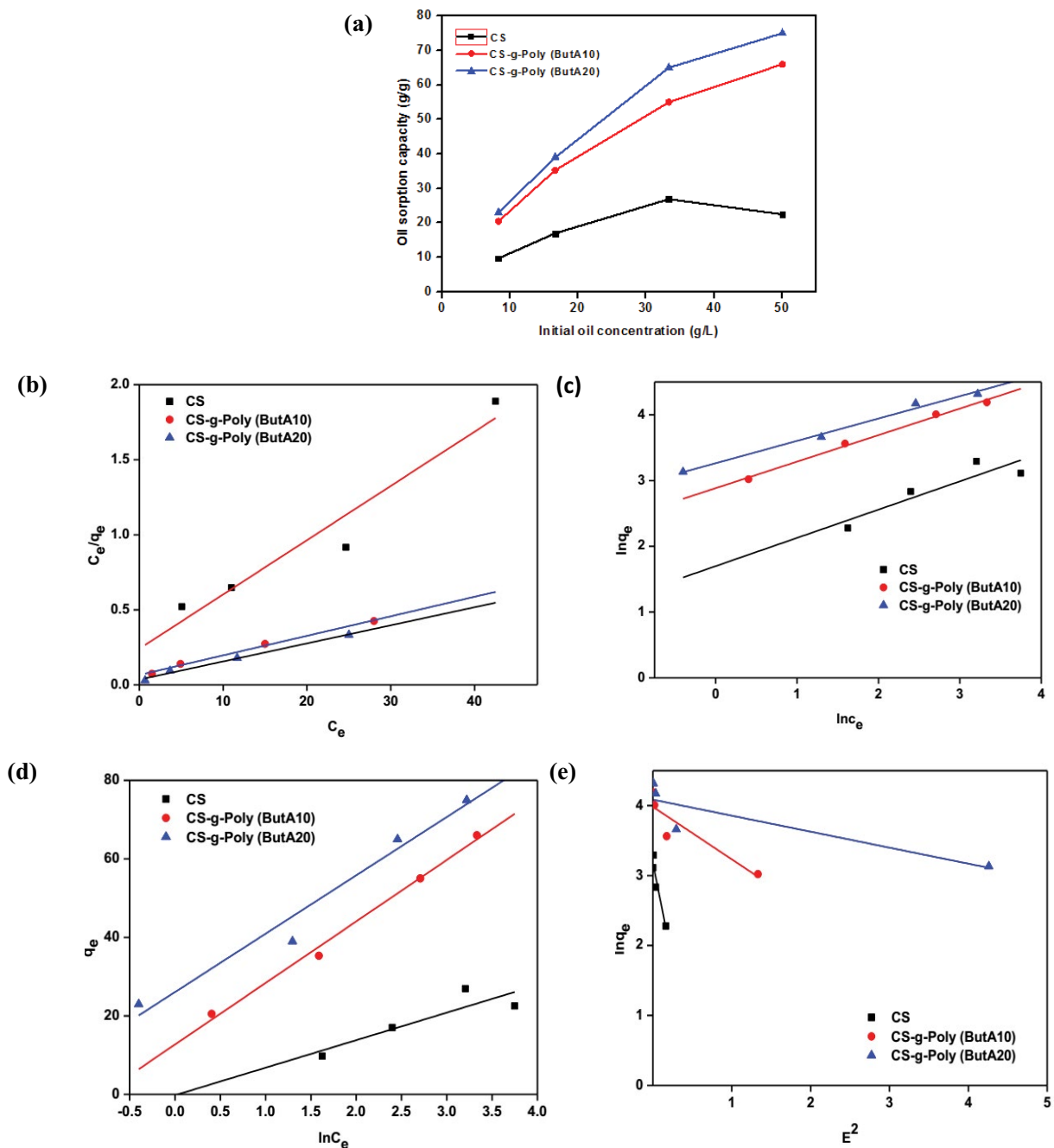
Fig. 4. (a) Effect of the initial crude oil concentration on the sorption equilibrium, (b–e) equilibrium isotherm for the sorption of the crude oil onto the prepared chitosan derivatives, (b) Langmuir, (c) Freundlich isotherm, (d) Temkin, and (e) Dubin–Radushkevich isotherm.

concentration of the oil residue in solute can strongly influence the sorption kinetics and more particularly the mechanism that regulates the overall kinetic coefficient. Fig. 4a reveals the relation between the initial oil concentration and the adsorbed amount by the CS and its grafted structures. The plots explain that the sorption of oil improves with increasing the initial oil concentration up to a certain level and attains equilibrium. The oil sorptive capacity increases dramatically after the modification with ButA due to the presence of hydrophobic groups from ButA [38].

Furthermore, Grafted poly (ButA) is oleophilic, and its incorporation onto CS makes CS-g-poly (ButA) copolymer lipophilic. Indeed, at higher concentration, the gradient between the bulk solution and the centre of sorbent particle improves the oil residue distribution through the film surrounding the particle and in the interior network of the prepared sorbents, as well, high sorption rate and proper consumption of available vacant sites [39].

Sorption isotherms are used to explicate the nature of sorption and interaction between the quantity adsorbed

and initial crude oil concentrations, as well as the existing equilibrium between adsorbent and adsorbate [37]. Therefore, sorption isotherms are critical in optimizing the use of adsorbents.

In this research, four well-known sorption isotherm shapes have used to fit the experimental data. The linear equation of Langmuir (Eq. (11)), Freundlich (Eq. (12)), Temkin (Eq. (13)), and Dubin-Radushkevich (D–R) (Eq. (14)) isotherm models are given as [37,51]:

$$\frac{C_e}{q_e} = \frac{1}{q_{max}K_L} + \frac{C_e}{q_{max}} \tag{11}$$

$$\ln q_e = \ln K_F + \frac{1}{n}\ln C_e \tag{12}$$

$$q_e = B_T \ln KT + B_T \ln C_e \tag{13}$$

$$\ln q_e = \ln q_{D-R} - K_{ad}\varepsilon^2 \tag{14}$$

where $q_{max}$ (g/g), $C_e$ (g/L), and $K_L$ (L/g) are the saturated sorption capacity, the crude oil concentration at equilibrium, and the Langmuir isotherm constant, respectively, $1/n$ and $K_f$ are the Freundlich constants belonged to sorption intensity and sorption capacity. $B$ (J/mol) is the heat of sorption, and $K_T$ (L/g) is the highest binding energy of adsorbent and adsorbate.

These models are portrayed in Figs. 4b–e. The isotherm constants whose values signify the perceptivity of the adsorbate toward the surface of the sorbent is shown in Table 3. The high values of $q_{max}$ and the low values of $K_L$ obtained from the linear plot of the Langmuir model (Fig. 4b), illustrates that the synthesised CS and the grafted copolymers have a high affinity for crude oil (large organic molecules) as described earlier by Elanchezhiyan et al. [52]. Otherwise, the dimensionless separation factor ($R_L$) which

outline the fundamental characteristics of the Langmuir isotherm can be expressed by [53]:

$$R_L = \frac{1}{1 + K_L C_0} \tag{15}$$

For this sorption process, the $R_L$ values were $0 < R_L < 1$ and the values of $n$ were more significant than 1, demonstrating the favorable sorption of the crude oil on the CS adsorbents. This value suggests that the prepared CS samples are suitable adsorbents for the pickup of crude oil spills. Also, the $R^2$ value of the Langmuir isotherm for the CS adsorbent (0.94) is higher than the obtained value from the Freundlich (Fig. 4c) and D–R isotherm (Fig. 4e) models; proposing monolayer sorption with homogeneous sorption energy [37]. Oppositely, the $R^2$ values for CS-g- poly (ButA) copolymers are higher than 0.99 for both the Langmuir and the Freundlich isotherms describing that monolayer and multilayer sorption played a crucial role in the crude oil-uptake on the grafted copolymers. The maximum monolayer sorption capacities were obtained to be 27.7 for native CS while reaching higher values of 76.9 and 83.3 g/g for CS-g- poly (ButA10) and CS-g-poly (ButA20) copolymers.

Furthermore, the positive and higher values of the $B_T$ parameter obtained from the Temkin plot (Fig. 4d) indicate the higher adsorbent/adsorbate interaction. The Sorption energy ($E$) obtained from D–R isotherm was less than 8, indicating that the sorption of crude oil onto all CS sorbents was physisorption [14]. This observation, suggests that more than one mechanism governs the sorption process, and it agrees with other publication [40,54]. Moreover, the attained maximum monolayer sorption capacity for the sorption of crude oil onto the all prepared CS sorbents has been compared with the $q_{max}$ for other listed adsorbents (Table 4). It was evident that the grafted CS copolymers apparently exhibit higher performance than other

Table 3
Parameters of the different isotherm models and correlation coefficients for the sorption of the crude oil

| Sorbent type | | CS | CS-g-poly (ButA10) | CS-g-poly (ButA20) |
|---|---|---|---|---|
| Isotherm | Parameters | Values | | |
| Langmuir | $q_{max}$ (g/g) | 27.70 | 76.60 | 83.30 |
| | $K_L$ (L/g) | 0.14 | 0.19 | 0.33 |
| | $R^2$ | 0.94 | 0.99 | 0.99 |
| Freundlich | $K_f$ (g/g) | 4.60 | 7.80 | 8.80 |
| | $1/n$ | 0.43 | 0.40 | 0.33 |
| | $R^2$ | 0.81 | 0.99 | 0.99 |
| Temkin | $K_T$ (L/g) | 0.08 | 2.20 | 4.70 |
| | $B$ (J/mol) | 7.52 | 10.82 | 12.99 |
| | $R^2$ | 7 | 15.60 | 14.80 |
| D–R | $K_{ad}$ (mol²/KJ²) | 5.37 | 4.93 | 2.93 |
| | $E$ (KJ/mol) | 0.29 | 0.81 | 1.47 |
| | $R^2$ | 0.92 | 0.84 | 0.78 |

(a)



(b)
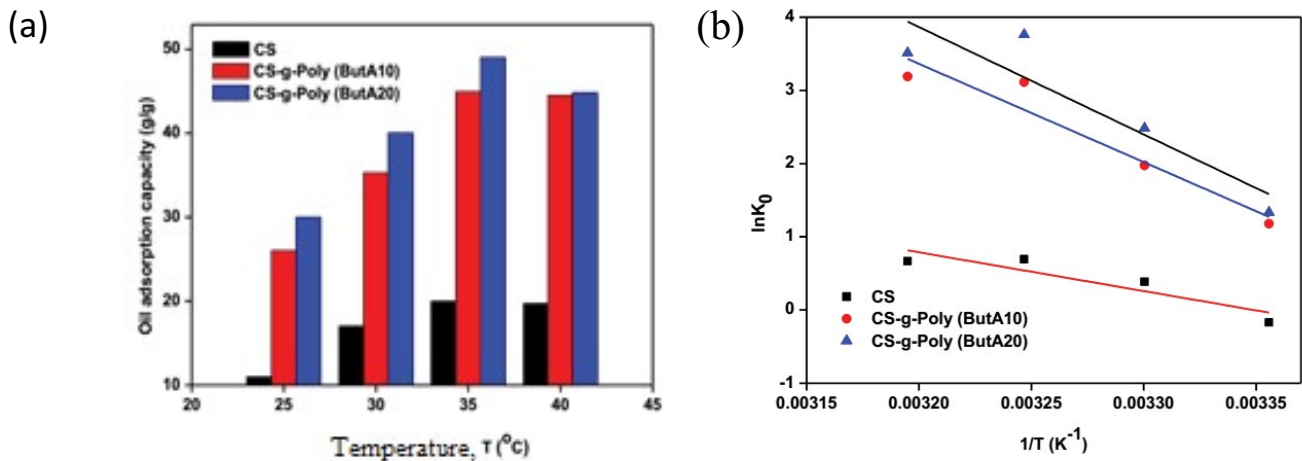


Fig. 5. Thermodynamics of the sorption of the crude oil onto the prepared chitosan derivatives. (a) $T$ (°C) and (b) $1/T$ (K$^{-1}$).

adsorbents earlier reported. However, this comparison is unfair owing to the diversity of the operating conditions.

### 3.3.5. Effect of sorption temperature and thermodynamics parameters

The behavior of the oil sorption onto the prepared sorbents was estimated under various sorption temperatures extended from 25°C to 40°C as conferred in Fig. 5a. It was understandable from the consequences that the sorption capacity was enhanced by elevating temperature from 25°C to 35°C and later tends to reduce with an extra acceleration of temperature to 40°C. These results could be described by promoting the segmental movement for all analysed adsorbents, where the distribution rate of spillage oil into the sorbent surface enhanced with raising the temperature to 35°C. Although, the increase of temperature exceeding 35°C (up to 40°C) could accelerate the rate of Brownian movement of the sorption medium. Thus higher energy is obliged to adhere the oil molecules onto the sorbent surface [51]. Hence, raised temperature induces less possibility of oil attachment on the sorbent surface, and the oil desorption could befall. Furthermore, the oil viscosity drop at elevated temperatures and the oil solubility increased, so, the sorption capacity values reduced consequently. A similar investigation were confirmed [40,51].

Table 4
Comparison of the maximum sorption capacity for the crude oil by various sorbents

| Adsorbent | Sorption capacity/ Removal efficiency | Reference |
|---|---|---|
| Chitosan flakes | 0.38 g/g | [55] |
| Chitosan powder | 0.28 g/g | [55] |
| Chitosan-based polyacrylamide hydrogel | 2.31 g/g | [31] |
| Chitosan (prawn shells( | 18.52 g/g | [56] |
| Chitosan-coated mesh | >99% | [56] |
| Chitosan based aerogel membrane | 99% | [58] |
| Chitosan microspheres | >90% | [59] |
| Acetylated corncobs | 0.08 mg/g | [60] |
| Lauric acid (LA) modified oil palm leaves | 1.2 ± 0.12 mg/g | [13] |
| Carbonized rice husks (CRH) | 6 g/g | [13] |
| Cellulose aerogel functionalized with methyltrimethoxysilane | 24.41 g/g | [61] |
| Butyl rubber | 25 g/g | [10] |
| Non-woven polypropylene | 15 g/g | [10] |
| Biochar | 166 mg/g | [62] |
| BuAc cellusoe graft coplomer | 13.83 g/g | [32] |
| Chitosan | 27.70 g/g | This study |
| CS-g-poly (ButA10) | 76.90 g/g | This study |
| CS-g-poly (ButA20) | 83.30 g/g | This study |

Table 5
Thermodynamic parameters of the sorption capacity for the crude oil by various chitosan sorbents

| | Thermodynamic parameters | | | | | | | | |
|---|---|---|---|---|---|---|---|---|---|
| Sorbent type | CS | | | CS-g-poly(ButA10) | | | CS-g-poly(ButA20) | | |
| $T$ (K) | $\Delta G$ (kJ/mol) | $\Delta H$ (kJ/mol) | $\Delta S$ (J/mol K) | $\Delta G$ (kJ/mol) | $\Delta H$ (kJ/mol) | $\Delta S$ (J/mol K) | $\Delta G$ (kJ/mol) | $\Delta H$ (kJ/mol) | $\Delta S$ (J/mol K) |
| 298 | −0.44 | | | −0.36 | | | −1.56 | | |
| 303 | −1.18 | 43.98 | 147.29 | −0.11 | 111 | 384 | −1.91 | 121 | 422 |
| 308 | −1.93 | | | −1.68 | | | −2.26 | | |
| 313 | −2.68 | | | −2.34 | | | −2.61 | | |

The spontaneity of the sorption process can be considered by the thermodynamic parameters, the enthalpy ($\Delta H$), the entropy ($\Delta S$) and the free energy change ($\Delta G$) which determined using the next Eqs. (16) and (17) [40]:

$$K_D = \frac{Q_e}{C_e} \tag{16}$$

$$\ln K_D = -\frac{\Delta H}{RT} + \frac{\Delta S}{R} \tag{17}$$

where $\Delta G$ and $\Delta H$ are in kJ/mol, $\Delta S$ is in J/mol K, $T$ is the sorption temperature in K, and $R$ is the universal gas constant (8.314 J/mol).

Thermodynamic parameters reviewed in Table 5 can be investigated from the incline and intercept of the plot of $\ln K_D$ vs $1/T$ given in Fig. 5b. The received $\Delta G$ values for the all used sorbents were negatively informed that sorption was spontaneous. Additionally, the variance of the $\Delta G$ diminishes with escalating temperatures regardless of the nature of sorbent. The positive values for the $\Delta H$ designate that the sorption is endothermic, which describes the increase of oil sorption capacity by elevating the temperature [51]. It was also approved that the sorption was complex with simultaneous chemical and physical reactions. However, the positive values of $\Delta S$ intends the increase in randomness at the adsorbent/adsorbed interface during the sorption process [63].

### 3.4. Oil sorption mechanism

Based on the kinetic study, the chemisorption mechanism plays a vital role in the sorption process of crude oil onto the prepared sorbents. Besides, the oil sorption rate was significantly enhanced upon the modification of CS. Besides, the intraparticle-diffusion is not the only rate-determining step, while the film-diffusion is the rate-controlling mechanism. Furthermore, the results indicated that the sorption process was involved in nature with simultaneous chemical and physical reactions, spontaneous, and endothermic.

### 4. Conclusion

The present study built sorption kinetics and isotherms models as well as the thermodynamics of the sorption of heavy crude oil onto CS and CS grafted copolymers.

The as-prepared CS oil sorbents are natural, renewable, biodegradable and low-cost materials. Kinetics investigation confirmed that the sorption process best fitted the pseudo-second-order model. The Elovich and the intraparticle diffusion models imply that more than one mechanism was incorporated in the sorption system. Langmuir isotherm best define the sorption of oil spills onto CS. While, both the Langmuir and the Freundlich isotherms best describe the sorption behaviour onto CS grafted copolymers. However, the initial rapid sorption rate was onto a uniform homogenous site thus maximum monolayer sorption capacity was obtained to be 27.7, 76.9, and 83.3 g/g for CS, CS-g- poly (ButA10), and CS-g-poly (ButA20), respectively. The thermodynamics parameters designate that the sorption manner is spontaneous, endothermic, and included both physical and chemical reactions. Compared with other modified adsorbents, the present economic and eco-friendly grafted modified chitosan shows sufficient buoyancy and excellent potential for the cleanup of leaked oil from the polluted surface.

### References

[1] H.I. Kelle, Mopping of crude oil and some refined petroleum products from the environment using sawmill factory waste: adsorption isotherm and kinetic studies, J. Appl. Sci. Environ. Manage., 22 (2018) 34–40.

[2] Q. Hao, Y. Song, Z. Mo, S. Mishra, J. Pang, Y. Liu, J. Lian, J. Wu, S. Yuan, H. Xu, Highly efficient adsorption of oils and pollutants by porous ultrathin oxygen-modified BCN nanosheets, ACS Sustainable Chem. Eng., 7 (2019) 3234–3242.

[3] E.T. Nwankwere, C.E. Gimba, G.I. Ndukwe, A.K. Isuwa, Modeling of the kinetic and equilibrium sorption behavior of crude oil on HDTMAB modified nigerian nanoclays, Int. J. Sci. Technol. Res., 4 (2015) 106–114.

[4] G. Ju, J. Liu, D. Li, M. Cheng, F. Shi, Chemical and equipment-free strategy to fabricate water/oil separating materials for emergent oil spill accidents, Langmuir, 33 (2017) 2664–2670.

[5] O. Carmody, R. Frost, Y. Xi, K. Serge, Adsorption of hydrocarbons on organo-clays-implications for oil spill remediation, J. Colloid Interface Sci., 305 (2007) 17–24.

[6] B.T. Song, Q. Xu, Highly hydrophobic and superoleophilic nanofibrous mats with controllable pore sizes for efficient oil/water separation, Langmuir, 32 (2016) 9960–9966.

[7] B. Doshi, M. Sillanpää, S. Kalliola, A review of bio-based materials for oil spill treatment, Water Res.,135 (2018) 262–277.

[8] R.K. Gupta, G.J. Dunderdale, M.W. England, A. Hozumi, Oil/water separation techniques: a review of recent progresses and future directions, J. Mater. Chem. A, 5 (2017) 16025–16058

[9] Q.F. Wei, R.R. Mather, A.F. Fotheringham, R.D. Yang, Evaluation of nonwoven polypropylene oil sorbents in marine oil-spill recovery, Mar. Pollut. Bull., 46 (2003) 780–783.

[10] D. Ceylan, S. Dogu, B. Karacik, S.D. Yakan, O.S. Okay, O. Okay, Evaluation of butyl rubber as sorbent material for the removal of oil and polycyclic aromatic hydrocarbons from seawater, Environ. Sci. Technol., 43 (2009) 3846–3852.

[11] M. Keshawy, T.A. El-Moghny, A-R.M. Abdul-Raheim, K. Kabel, S.H. El-Hamouly, Synthesis and characterization of oil sorbent based on hydroxypropyl cellulose acrylate, Egypt. J. Pet., 22 (2013) 539–548.

[12] P. Venkataraman, J. Tang, E. Frenkel, G.L. McPherson, J. He, S.R. Raghavan, V. Kolesnichenko, A. Bose, V.T. John, Attachment of a hydrophobically modified biopolymer at the oil-water interface in the treatment of oil spills, ACS Appl. Mater. Interfaces, 5 (2013) 3572–3580.

[13] S.M. Sidik, A.A. Jalil, S. Triwahyono, S.H. Adam, M.A.H. Satar, B.H. Hameed, Modified oil palm leaves adsorbent with enhanced hydrophobicity for crude oil removal, Chem. Eng. J., 203 (2012) 9–18.

[14] H.H. Sokker, N.M. El-Sawy, M.A. Hassan, B.E. El-Anadouli, Adsorption of crude oil from aqueous solution by hydrogel of chitosan based polyacrylamide prepared by radiation induced graft polymerization, J. Hazard. Mater., 190 (2011) 359–365.

[15] S. Li, Y. Gao, H. L. Bai, L.P. Zhang, P. Qu, L. Bai, Preparation and characteristics of poly sulfone dialysis composite membranes modified with nanocrystalline cellulose, Bioresources, 6 (2011) 1670–1680.

[16] P. Qu, Y. Gao, G.F. Wu, L.P. Zhang, Nanocomposites of poly (lactic acid) reinforced with cellulose nanofibrils, Bioresources, 5 (2010) 1811–1823.

[17] P. Qu, H.W. Tang, Y. Gao, L.P. Zhang, S.Q. Wang, Polyethersulfone composite membrane blended with cellulose fibrils, Bioresources, 5 (2010) 2323–2336.

[18] G.S. Chauhan, B. Singh, S. Kumar, A. Chinkara, Synthesis and characterization of reactive copolymers of poly (butyl acrylate) and celluose, Polym. Polym. Compos., 13 (2005) 467–477.

[19] M.S. Mohy Eldin, Y.A. Ammar, T.M. Tamer, A.M. Omer, A.A. Ali, Development of low-cost chitosan derivatives based on marine waste sources as oil adsorptive materials: i. preparation and characterization, Desal. Water Treat., 72 (2017) 41–51.

[20] M.S. Mohy Eldin, Y.A. Ammar, T.M. Tamer, A.M. Omer, A.A. Ali, Development of oleophilic adsorbent based on chitosan- poly (butyl acrylate) graft copolymer for petroleum oil spill removal, Int. J. Adv. Res., 4 (2016) 2095–2111.

[21] S.W. Benner, V.T. John, C.K. Hall, Simulation study of hydrophobically modified chitosan as an oil dispersant additive, J. Phys. Chem. B, 119 (2015) 6979–6990.

[22] M.T. Tamer, V. Katarína, A.H. Mohamed, M.O. Ahmed, E.-S. Muhammad, S.M.-E. Mohamed, Š. Ladislav, Chitosan/ hyaluronan/edaravone membranes for anti-inflammatory wound dressing: in vitro and in vivo evaluation studies, Mater. Sci. Eng., C, 90 (2018) 227–235.

[23] H. Honarkar, M. Barikani, Applications of biopolymers i: chitosan, Monatsh. Chem., 140 (2009) 1403–1420.

[24] X.X. Liang, A.M. Omer, Z. Hu, Y. Wang, D. Yu, X. Ouyang, Efficient adsorption of diclofenac sodium from aqueous solutions using magnetic amine-functionalized chitosan, Chemosphere, 217 (2018) 270–278.

[25] A. Eskhan, F. Banat, M. Abu Haija, S. Al-Asheh, Synthesis of mesoporous/macroporous microparticles using three-dimensional assembly of chitosan-functionalized halloysite nanotubes and their performance in the adsorptive removal of oil droplets from water, Langmuir, 35 (2019) 2343–2357.

[26] D.W. Jenkins, M.H. Samuel, Review of vinyl graft copoly-merization featuring recent advances toward controlled radical-based reactions and illustrated with chitin/chitosan, Trunk Polymers, Chem. Rev.,101 (2001) 3245–3273.

[27] R. Nithya, P.N. Sudha, Grafting of N-butyl acrylate on to chitosan by ceric Ion initiation and its antimicrobial activity, Der Pharm. Lett., 6 (2014) 58–64.

[28] V.K. Mourya, N.N. Inamdar, Chitosan-modifications and applications: opportunities galore, React. Funct. Polym., 68 (2008)1013–1051.

[29] M.S. Mohy Eldin, H.M. El-Sherif, E.A. Soliman, A.A. Elzatahry, A.M. Omer, Polyacrylamide-grafted carboxymethyl cellulose: smart pH-sensitive hydrogel for protein concentration, J. Appl. Polym. Sci., 12 (2011) 469–479.

[30] A.H. Mohamed, M.O. Ahmed, A. Eman, M.A.B. Walid, M.T. Tamer, Preparation, physicochemical characterization and antimicrobial activities of novel two phenolic chitosan Schiff base derivatives, Sci. Rep., 8 (2018) 1–14.

[31] A. Bazargan, J. Tan, G. McKay, Standardization of oil sorbent performance testing, J. Test. Eval., 43 (2015) 1–10.

[32] G. Yuan, Z. Yitong, Z. Xiaoli, Z. Liping, Q. Ping, Synthesis and characteristics of graft copolymers of poly(butyl acrylate) and cellulose fiber with ultrasonic processing as a material for oil absorption, Bioresources, 7 (2012) 135–147.

[33] N. Ibrahim, W.W. Yunus, F. Abu-Ilaiwi, M. Rahman, M. Ahmad, K. Dahlan, Optimized condition for grafting reaction of poly(butyl acrylate) onto oil palm empty fruit bunch fibre, Polym. Int., 52 (2003) 1119–1124.

[34] T.M. Tamer, W.M. Abou-Taleb, G.D. Roston, M.S. Mohyeldin, A.M. Omer, R.E. Khalifa, A.M. Hafez, Formation of zinc oxide nanoparticles using alginate as a template for purification of wastewater, Environ. Nanotechnol. Monit. Manage., 10 (2018)112–121.

[35] A.M. Omer, R.E. Khalifa, Z. Hu, H. Zhang, C. Liu, X.K. Ouyang, Fabrication of tetraethylenepentamine functionalized alginate beads for adsorptive removal of Cr(VI) from aqueous solutions, Int. J. Biol. Macromol, 125 (2019) 1221–1231.

[36] R.E. Khalifa, A.M. Omer, T.M. Tamer, A.A. Ali, Y.A. Ammar, M.S. Mohy Eldin, Efficient eco-friendly crude oil adsorptive chitosan derivatives: kinetics, equilibrium and thermodynamic studies, Desal. Water. Treat., (2019) 1–13.

[37] R.E. Khalifa, A.M. Omer, T.M. Tamer, W.M. Salem, M.S. Mohy Eldin, Removal of methylene blue dye from synthetic aqueous solutions using novel phosphonate cellulose acetate membranes: adsorption Kinetic, equilibrium, and thermodynamic studies, Desal. Water. Treat., 144 (2019) 272–285.

[38] A. Ummadisingu, S. Gupta, Characteristics and kinetic study of chitosan prepared from seafood industry waste for oil spills cleanup, Desal. Water Treat., 44 (2012), 44–51.

[39] N.E. Thompson, G.C. Emmanuel, K.J. Adagadzu, N.B. Yusuf, Sorption studies of crude oil on acetylated rice husks, Arch. Appl. Sci. Res., 2 (2010) 142–151.

[40] H. Li, X. Zhuang, M. Bao, Kinetics and thermodynamics of dissolved petroleum hydrocarbons in sediment under sophorolipid application and their effects on oil behavior end-results in marine environment, RSC Adv., 7 (2017) 45843–45851.

[41] Z. Li, B. Wang, X. Qin, Y. Wang, C. Liu, Q. Shao, N. Wang, J. Zhang, Z. Wang, C. Shen, Superhydrophobic/superoleophilic polycarbonate/carbon nanotubes porous monolith for selective oil adsorption from water, ACS Sustainable Chem. Eng., 6 (2018) 13747–13755.

[42] S.M. Davoodi, M. Taheran, S.K. Brar, R. Galvez-Cloutier, R. Martel, Hydrophobic dolomite sorbent for oil spill clean-ups: kinetic modeling and isotherm study, Fuel, 251 (2019) 57–72.

[43] S.C, Cheu, H. Kong, S.T. Song, K. Johari, N. Saman, M.A.C. Yunus, Separation of dissolved oil from aqueous solution by sorption onto acetylated lignocellulosic biomass: equilibrium, kinetics and mechanism Studies, J. Environ. Chem. Eng., 4 (2016) 868–881.

[44] Z. Wang, J.P. Barford, C.W. Hui, G. Mckay, Kinetic and equilibrium studies of hydrophilic and hydrophobic rice husk cellulosic fibers used as oil spill sorbents, Chem. Eng. J., 281 (2015) 961–969.

[45] F.C. Wu, R.L. Tseng, R.S. Juang, Characteristics of elovich equation used for the analysis of adsorption kinetics in dye-chitosan systems, Chem. Eng. J., 150 (2009) 366–373.

[46] Ş. Taşar, F. Kaya, A. Özer, Biosorption of lead(II) ions from aqueous solution by peanut shells: equilibrium, thermodynamic and kinetic studies, J. Environ. Chem. Eng., 2 (2014) 1018–1026.

[47] A.U. Itodo, F.W. Abdulrahman, L.G. Hassan, S.A. Maigandi, H.U. Itodo, Intraparticle diffusion and intraparticulate

diffusivities of herbicide on derived activated carbon, Research, 2 (2010) 74–86.

[48] D.C. Sinica, C. Imaga, A.A. Abia, J.C. Igwe, Removal of Ni(II), Cu(II) and Zn(II) ions from synthetic wastewater using sorghum hulls as adsorbents, Der Chem. Sin., 5 (2014) 67–75.

[49] M.A. Ahmad, P.N.A. Ahmad, O.S. Bello, Kinetic, equilibrium and thermodynamic studies of synthetic dye removal using pomegranate peel activated carbon prepared by microwave-induced KOH activation, Water Resour. Ind., 6 (2014)18–35.

[50] S. Karthikeyan, B. Sivakumar, N. Sivakumar, Film and pore diffusion modeling for adsorption of reactive red 2 from aqueous solution on to activated carbon prepared from bio-diesel industrial waste, J. Chem., 7 (2012) S175-S184.

[51] A. Achmad, J. Kassim, T.K. Suan, R.C. Amat, T.L. Seey, Equilibrium, kinetic and thermodynamic studies on the adsorption of direct dye onto a novel green adsorbent developed from uncaria gambir extract, J. Phys. Sci., 23 (2012) 1–13.

[52] S.S. Elanchezhiyan, N. Sivasurian, S. Meenakshi, Enhancement of oil recovery using zirconium-chitosan hybrid composite by adsorptive method, Carbohydr. Polym., 145 (2016) 103–113.

[53] I.D. Mall, V.C. Srivastava, N.K. Agarwal, I.M. Mishra, Removal of congo red from aqueous solution by bagasse fly ash and activated carbon: kinetic study and equilibrium isotherm analysis, Chemosphere, 61 (2005) 492–501.

[54] S.S. Elanchezhiyan, S. Meenakshi, Synthesis and characterization of chitosan/Mg-Al layered double hydroxide composite for the removal of oil particles from oil-in-water emulsion, Int. J. Biol. Macromol., 104 (2017) 1586–1595.

[55] F.C.F. Barros, L. Vasconcellos, C. Grombone, T.V. Carvalho, R.F.D. Nascimento, Removal of petroleum spill in water by chitin and chitosan, Orbital Electron. J. Chem., 6 (2014) 70–74.

[56] V.K. Gupta, A. Mittal, A. Malviya, J. Mittal, Adsorption of carmoisine A from wastewater using waste materials-bottom ash and deoiled soya, J. Colloid. Interface. Sci., 335 (2009) 24–33.

[57] S. Zhang, F. Lu, L. Tao, N. Liu, C. Gao, L. Feng, Y. Wei, Bio-inspired anti-oil-fouling chitosan-coated mesh for oil/water separation suitable for broad pH range and hyper-saline environments, ACS Appl. Mater. Interfaces, 5 (2013) 11971–11976

[58] J.P. Chaudhary, N. Vadodariya, S.K. Nataraj, R. Meena, Chitosan-based aerogel membrane for robust oil-in-water emulsion separation, ACS Appl. Mater. Interfaces, 7 (2015) 24957–24962.

[59] I.C.S. Grem, B.N.B. Lima, W.F. Carneiro, Y.G.C. Queirós, C.R.E. Mansur, Chitosan microspheres applied for removal of oil from produced water in the oil industry, Polímeros. Ciência. Tecnol., 23 (2013) 705–711.

[60] J.O. Nwadiogbu, V.I.E. Ajiwe, P.A.C. Okoye, Removal of crude oil from aqueous medium by sorption on hydrophobic corncobs: equilibrium and kinetic studies, J. Taibah Univ. Sci., 10 (2015) 56–63.

[61] T.N. Son, F. Jingduo, T.L. Nhat, T.T.L. Ai, H. Nguyen, B.C.T. Vincent, M.D. Hai, Cellulose aerogel from paper waste for crude oil spill cleaning, Ind. Eng. Chem. Res., 52 (2013) 18386–18391.

[62] L. Silvani, B. Vrchotova, P. Kastanek, K. Demnerova, I. Pettiti, M.P. Papini, Characterizing biochar as alternative sorbent for oil spill remediation, Sci. Rep., 7 (2017) 1–10.

[63] N. Lv, X. Wang, S. Peng, H. Zhang, L. Luo, Study of the kinetics and equilibrium of the adsorption of oils onto hydrophobic jute fiber modified via the sol-gel method, Int. J. Environ. Res. Public Health, 15 (2018) 969–983.